Joint inversion of long-period magnetotelluric data and surface-wave dispersion curves for anisotropic structure: Application to data from Central Germany

E. Roux,[1,2] M. Moorkamp,[3] A. G. Jones,[1] M. Bischoff,[4] B. Endrun,[5] S. Lebedev,[1] and T. Meier[6]

Received 30 November 2010; revised 25 January 2011; accepted 2 February 2011; published 10 March 2011.

[1] Geophysical datasets sensitive to different physical parameters can be used to improve resolution of Earth's internal structure. Herein, we jointly invert long-period magnetotelluric (MT) data and surface-wave dispersion curves. Our approach is based on a joint inversion using a genetic algorithm for a one-dimensional (1-D) isotropic structure, which we extend to 1-D anisotropic media. We apply our new anisotropic joint inversion to datasets from Central Germany demonstrating the capacity of our joint inversion algorithm to establish a 1-D anisotropic model that fits MT and seismic datasets simultaneously and providing new information regarding the deep structure in Central Germany. The lithosphere/asthenosphere boundary is found at approx. 84 km depth and two main anisotropic layers with coincident most conductive/seismic fast-axis direction are resolved at lower crustal and asthenospheric depths. We also quantify the amount of seismic and electrical anisotropy in the asthenosphere showing an emerging agreement between the two anisotropic coefficients. **Citation:** Roux, E., M. Moorkamp, A. G. Jones, M. Bischoff, B. Endrun, S. Lebedev, and T. Meier (2011), Joint inversion of long-period magnetotelluric data and surface-wave dispersion curves for anisotropic structure: Application to data from Central Germany, *Geophys. Res. Lett.*, *38*, L05304, doi:10.1029/2010GL046358.

1. Introduction

[2] The main discontinuities in the Earth's crust and upper mantle, namely the crust-mantle boundary (geophysically identified as the Moho) and the Lithosphere/Asthenosphere Boundary (LAB), correspond to physical and compositional changes of minerals. These two main interfaces are, to varying degrees, sensed by both seismology and magnetotellurics [*Jones and Ferguson*, 2001; *Jones et al.*, 2003] and we can thus expect to improve our models of the upper mantle when combining these two datasets.

[3] On the basis of observations, the electric LAB (eLAB) is described as a transition between a resistive lithosphere and a more conductive layer at upper mantle depths, taken to be the asthenosphere. Similarly, one definition of the seismological characterization of the LAB (sLAB) is the transition to a low-velocity zone underlying a relatively high velocity lithospheric lid. The sLAB has also been defined as a transition between a fossil and present-day flow-related anisotropy [*Eaton et al.*, 2009].

[4] Upper mantle seismic anisotropy is most-often interpreted to be controlled by lattice-preferred orientation of olivine crystals, which is the most abundant mineral in the lithosphere [*Savage*, 1999]. Surface waves (SW) have proven to be well suited for isotropic and anisotropic investigations at lithospheric scale [*Deschamps et al.*, 2008]. Fundamental-mode Rayleigh wave dispersion curves can be inverted for Vs models and azimuthal variations of Rayleigh phase velocities can constrain azimuthal anisotropy with good vertical resolution.

[5] The origin of electrical anisotropy in the upper mantle is more controversial, mainly because the observed anisotropy is significantly higher than predicted from intrinsic crystal anisotropy of dry mantle minerals. Indeed, dry olivine is only weakly anisotropic (factor of three at most [*Constable et al.*, 1992]) and other processes have been introduced to explain such a large anisotropy [*Simpson*, 2002; *Gatzemeier and Moorkamp*, 2005]. The presence of bound water is currently the most favored candidate to enhance conductivities and anisotropy, enabling the diffusion of hydrogen [*Karato*, 1990]. Additionally, the presence of other high conductive mineral phases, such as graphite [*Duba and Shankland*, 1982], has been proposed to enhance upper mantle conductivity.

[6] Despite these difficulties in interpretation and in understanding the origin of electrical anisotropy, an approximate agreement between the most conductive direction and the seismic fast axis direction has been found in several regions [*Simpson*, 2002; *Eaton et al.*, 2004], suggesting that, in some cases, a common underlying origin is likely for both seismic and electrical anisotropy. This motivates our attempt to invert jointly MT and SW data for 1-D azimuthally anisotropic structure.

[7] We apply an anisotropic joint inversion to two datasets from Central Germany. In this region, an independent magnetotelluric (MT) experiment suggested an eLAB at about 100 km depth [*Gatzemeier and Moorkamp*, 2005]. A seismic study based on inversion of SW fundamental modes resolved a pronounced low-velocity zone between approximately 80 and 200 km depth, interpreted as the asthenosphere [*Bischoff*

[1]Dublin Institute for Advanced Studies, Dublin, Ireland.
[2]Now at Institut de Ciències del Mar, CSIC, Barcelona, Spain.
[3]Leibniz Institute of Marine Sciences at University of Kiel (IFM-GEOMAR), Kiel, Germany.
[4]Institute of Geology, Mineralogy and Geophysics, Ruhr-University, Bochum, Germany.
[5]Institute of Earth and Environmental Sciences, University Potsdam, Potsdam, Germany.
[6]Institute of Geosciences, Christian-Albrechts University, Kiel, Germany.

0094-8276/11/2010GL046358

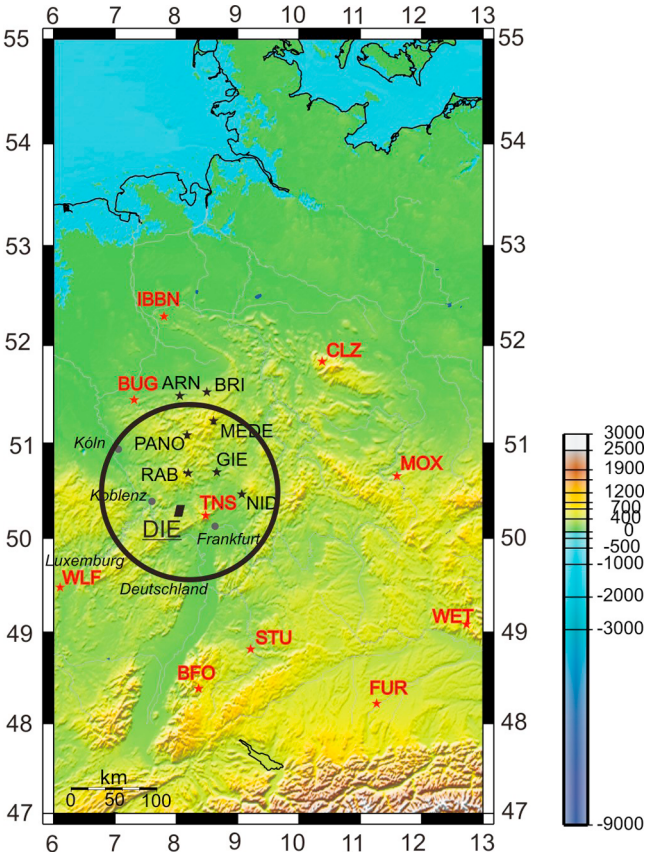

Figure 1. Topographic map of the region of study. Red stars show the seismic stations from the German Regional Seismic Network (GRSN) and black stars are the MT sites deployed between 1999 and 2000 discussed by *Gatzmeier and Moorkamp* [2005]. Here, we are inverting measurements from the MT site DIE together with four SW dispersion curves at different azimuths (15°, 44°, 96°, 152°). The circle represents the region sampled by the SW dispersion curves used in this study.

et al., 2006]. Recent estimates from S receiver functions put sLAB in the area between 80 and 100 km depth [*Geissler et al.*, 2010].

[8] Anisotropic phase velocity maps beneath western and central Germany reveal the presence of two main anisotropic layers with distinct fast-propagation directions, NE-SW in the lower crust/upper mantle, and E-W at asthenospheric depths. Moreover, in both layers, the seismic fast-axis coincides with the most conductive direction [*Lebedev et al.*, 2007].

[9] While indicating the presence of multiple layers of anisotropy, phase-velocity maps do not give specific depth ranges of the layers. In this paper, we use a joint inversion of the SW and long-period MT datasets and determine the depth distribution of both seismic and electrical anisotropy. As a result, we also obtain an empirical relationship between the amplitudes of the two types of anisotropy.

2. Data and Inversion

2.1. Data

[10] Azimuthal seismic anisotropy has been constrained with fundamental mode Rayleigh wave data recorded by the German Regional Seismic Network (GRSN). The network consists of 16 permanent broadband stations (STS-2 seismometers) installed in the early 1990s (Figure 1). The inter-station dispersion curves were measured using the two-station method [*Meier et al.*, 2004] with the maximum inter-station azimuth deviation from the great circle path set at 7° and the minimum magnitude of events of Ms = 5. Phase velocities were recorded in broad period ranges, from 10 s to over 200 s, yielding vertical resolution down to 300 km [*Bischoff et al.*, 2006].

[11] To constitute our input dataset, we can either use measured dispersion curves for four paths available in this area or extract dispersion curves from anisotropic phase velocity maps [*Lebedev et al.*, 2007]. Both possibilities have been tested and yield similar results. For brevity, we will only show the results obtained with the dispersion curves computed from phase velocity maps. We could have used additional azimuths but four directions are sufficient to resolve the two main anisotropic directions.

[12] For MT, we use the long-period measurements presented by *Leibecker et al.* [2002] and *Gatzemeier and Moorkamp* [2005]. We examined different sites for data quality and selected their site DIE as input MT data for the joint inversion (Figure 1). This site shows the same characteristics as the other sites in the same region with good data quality. Moreover, the region around this site is relatively homogeneous according to the MT and seismic measurements, thus allowing for valid 1-D modeling.

2.2. Inversion

[13] Our approach to modeling these two datasets jointly is a stochastic search through the model space using a Genetic Algorithm (GA). The approach is based on our extension of the joint inversion algorithm for a 1-D isotropic structure using long-period MT data and teleseismic receiver functions developed by *Moorkamp et al.* [2007] and extended to include SW dispersion curves by *Moorkamp et al.* [2010].

[14] We jointly invert long-period MT data and Rayleigh wave dispersion curves for a 1-D azimuthally anisotropic structure. The connection between the electrical and seismic models is established by a geometrical constraint, namely the requirement of coincident interfaces, which is the lowest possible coupling between the two structures.

[15] Within each layer, the free parameters are electrical resistivity, shear-wave velocity and layer thickness. Resistivity and velocity are uniform in each layer but mutually independent, i.e., there is no assumed parametric coupling between them.

[16] We also define several parameters to model anisotropy. The anisotropic electrical coefficient is the ratio between the values of resistivity perpendicular to strike and along strike. The anisotropic seismic coefficient in each layer is the peak-to-peak amplitude of the Pi-periodic (2ψ) anisotropic seismic velocity variation divided by the isotropic-average velocity, adopting the formulation for a weakly anisotropic medium [*Smith and Dahlen*, 1973]. We do not assume any relationship between electrical and seismic anisotropy coefficients.

[17] We define the directions of anisotropy as the most conductive direction for the MT structure and the seismic fast axis direction with respect to seismic structure. We can invert either for the same direction of anisotropy to increase the coupling between both structures, or allow a difference between the two directions. Separate inversions of each

Table 1. Range of Variation for Each Inverted Parameter

Inversion Parameter	Upper Crust (Layer 1)	Upper Crust (Layer 2)	Lower Crust/Upper Lithosphere (Layer 3)	Mantle Lithosphere (Layer 4)	Asthenosphere (Layer 5)
Thickness (km)					
Min. thick.	1	5	10	20	20
Max. thick.	16	20	35	83	83
Δt	1	1	1	1	1
ΔVs (km/s)					
Min. Vs	2.50	2.50	3.00	3.00	3.00
Max. Vs	3.77	3.77	4.27	5.54	5.54
ΔVs	0.01	0.01	0.01	0.02	0.02
ρ (Ω.m)					
Min. res.	80	1	1	1	1
Max. res.	(fixed)	10^6	10^6	10^6	10^6
log($\Delta\rho$)		0.1	0.1	0.1	0.1
Anisotropy	No anisotropy	Electrical and seismic anisotropy allowed	Electrical and seismic anisotropy allowed	Electrical and seismic anisotropy allowed	Electrical and seismic anisotropy allowed
Δstrike		MT and seismic anisotropic directions can be different	MT and seismic anisotropic directions can be different	MT and seismic anisotropic directions coincide	MT and seismic anisotropic directions coincide

datasets show similar anisotropic directions at lithospheric and sub-lithospheric depths (see auxiliary material).[1] We thus decide to invert for the same anisotropic direction at lithospheric and sub-lithospheric depths and for different MT and seismic strikes at crustal depths (Table 1). This is also in agreement with prior independent MT [*Gatzemeier and Moorkamp*, 2005] and seismic [*Lebedev et al.*, 2007] studies in Central Germany.

[18] We choose the range of model parameters to include *a priori* information regarding the expected seismic and electrical structures. Short-period SW data (T < 25 s) indicate strong crustal anisotropy, so we model the upper crust with an isotropic upper layer overlying a possibly anisotropic lower layer. We use a limited range of variation for the thicknesses and Vs of these two layers. We define three possibly anisotropic layers with a larger range of variation for both their thicknesses and Vs within them (Table 1). From the bottom of the asthenospheric upper-mantle layer to 410 km depth (Vs fixed to 4.87 km/s at this depth), an isotropic Vs gradient is applied. Below 410 km depth, the seismic structure is not perturbed and is taken from the global reference model AK135 [*Kennett et al.*, 1995].

[19] To diminish the effect of static shifts on the MT data, we invert for the parameters of the MT phase tensor [*Caldwell et al.*, 2004] rather than the MT impedance tensor. As the phase tensor is mostly sensitive to vertical variation of resistivity and not absolute values, we scale the model by fixing the value of resistivity in the first layer to 80 Ω.m [*Gatzemeier and Moorkamp*, 2005].

[20] Due to the stochastic nature of the GA, each run yields a different set of solutions. It is thus necessary to perform several runs of the GA to check the robustness of the results. For brevity, we discuss in more details one single run but comparison with other inversions shows that the main structural features are consistent between the different runs.

3. Results From Central Germany

[21] We perform a joint inversion of the MT and seismic datasets using a population size (i.e., the number of models in each iteration) of 800 members for 200 iterations. The crossover probability (i.e., probability for two selected models to exchange their binary representation at a randomly chosen location) is set to 0.6 and the mutation probability (i.e., probability for one bit to change its value) to 0.2.

[22] To stabilize the inversion, we add to the objective function we are minimizing, a term that measures the difference in apparent resistivity between two adjacent layers. The objective function is the sum of the misfit function and the regularization term Σ ($\rho_i - \rho_{i-1}$), where i is the i^{th} layer.

[23] A GA provides an ensemble of final models which gives us an estimate of the resolution of each inversion parameter. We will discuss our preferred model A together with all models which are fitting the datasets within the error bars.

[24] When we compare these best models, we can identify the main structural elements that are consistently resolved for all the best solutions (Figures 2a and 2b). The well-fitting solutions show a range in the depth of the e/sLAB from 75 to 91 km depth, with a depth of 84 km for Model A which achieves the minimum total misfit. The LAB corresponds to the top of a low-velocity/high conductivity layer with also a marked change in anisotropy. The depth of this boundary is constrained primarily by the seismic dataset. Inversions of the MT data alone put an eLAB within a broad range between 65 and 110 km depth (see auxiliary material), due to the large errors on the long-period estimates. MT measurements optimally resolve the top of a conducting layer and its conductance (conductivity-thickness product [see, e.g., *Jones*, 1982], and the thickness of a resistive layer, providing complementary information to the seismic dataset.

[25] The MT structure shows two anisotropic layers (Figure 2a). The first anisotropic layer is at crustal depths (between 10 and 22 km depth for model A) with a NE/SW most-conductive direction (30°).

[26] A deeper anisotropic layer is resolved below the LAB, between 84 and 145 km depth for model A. This layer is characterized by a strong electrical anisotropy coefficient and an East-West most conductive direction (72° azimuth). The minimum value of apparent resistivity in this layer is highly consistent for all the solutions plotted in Figure 2a (ρ~8 Ω.m or Log(ρ) ~0.9) and is strongly constrained by the longest periods (T > 500 s), (Figure 3a).

[1] Auxiliary materials are available in the HTML. doi:10.1029/2010GL046358.

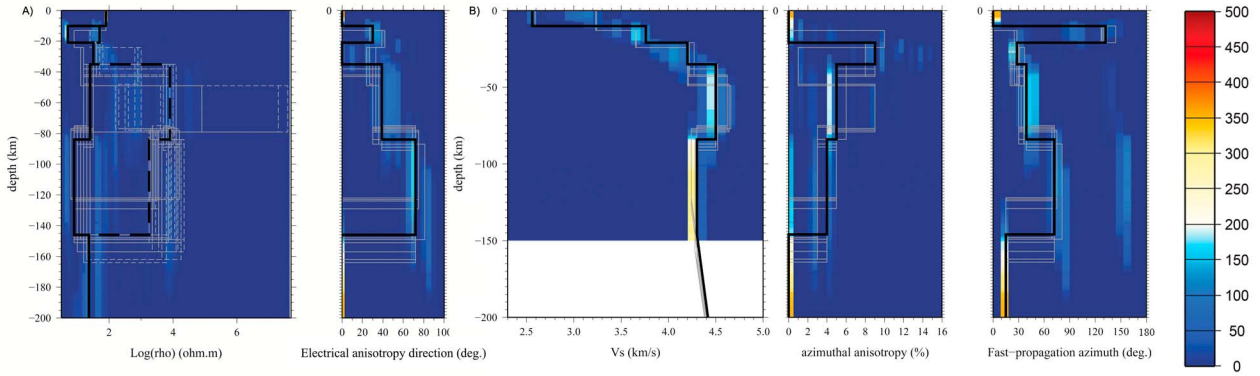

Figure 2. Joint MT and seismic models. (a) In black, minimum (solid lines) and maximum (dashed lines) values of resistivity on a logarithmic scale for our best model A. In grey, MT structure for all the solutions fitting the datasets within error bars. (b) Best solution (model A with black lines) and the best-fitting solutions given by the GA (grey lines). We plot the mean value of shear-wave velocity, the amount of azimuthal anisotropy and the fast-propagation azimuth. Also shown in Figure 2, a histogram that represents, for a certain depth, the number of models within a given interval for each inversion parameter. This plot takes into account all the performed GA runs.

[27] On the other hand, such a high maximum value of resistivity in the asthenosphere (Figure 2a) is not required. For an asthenospheric anisotropic direction of 72°, we show that the minimum amount of electrical anisotropy required between 84 km and 145 km depth to fit our data is about one order of magnitude (160 Ω.m/8 Ω.m).

[28] The well-fitting seismic models put strong azimuthal anisotropy between either 10 and 22 km depth or 22 and 35 km depth (Figures 2b and 3b). Such a strong seismic anisotropy coefficient is unusual but we can fit the data equally well by applying a smaller anisotropy coefficient in both layers. These best solutions thus indicate the presence of azimuthal anisotropy at lower-crustal/upper-lithospheric depths with a NE/SW fast axis direction (30°) and another layer of seismic anisotropy below 80 km depth, in the asthenosphere, with the fast axis turning east-westwards (Figure 2b).

4. Discussions and Conclusions

[29] Our anisotropic joint inversion of MT and SW measurements has enabled us to resolve a LAB lying between 75 and 91 km depth with a fast/resistive layer overlying a slow/conductive layer. This depth is shallower than that found by *Gatzemeier and Moorkamp* [2005] of 100 km, but, as noted above, the depth of this interface is mostly resolved

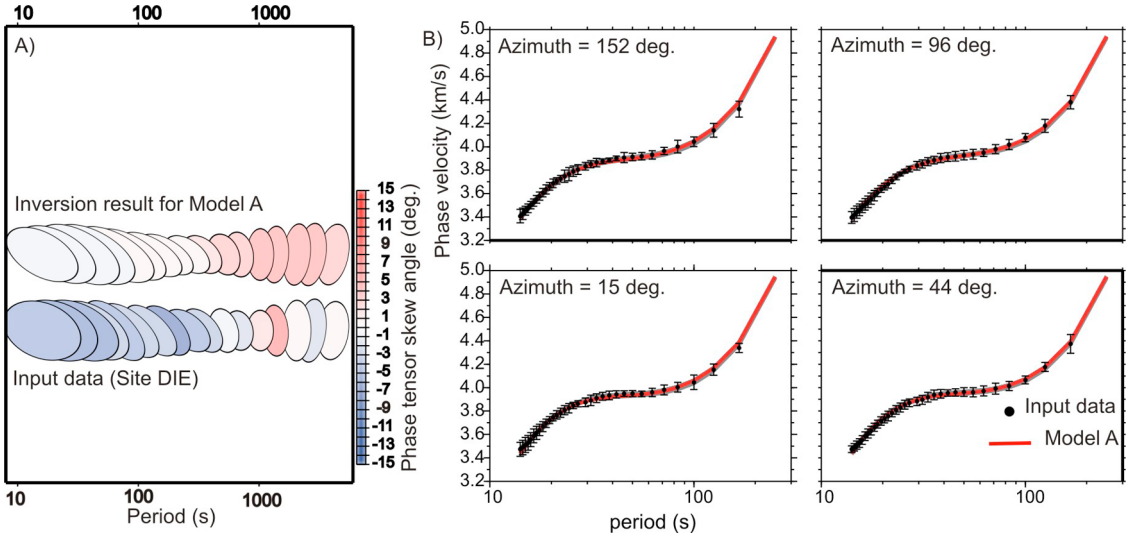

Figure 3. (a) Map view of the phase tensor ellipses at different periods for the input data (site DIE) and inversion result (Model A). The length of the ellipse's main axes are proportional to the principal axes of the tensor. Color of ellipses indicates the value of the skew (measures the asymmetry of the tensor). (b) Dispersion curves extracted from the anisotropic phase-velocity maps and showing phase velocities of Rayleigh wave at different azimuths (black dots) with their error bars. Red solid lines are the phase velocities computed for model A. In grey, dispersion curves computed for the set of solutions shown on Figure 2b.

by the seismic dataset and our result is fully consistent with previous seismic studies in this region [*Bischoff et al.*, 2006; *Geissler et al.*, 2010].

[30] As the resistivity in the resistive direction is virtually unbounded (statistically, not physically) on its upper end, we can only estimate a minimum value for the electrical anisotropy factor of about one order of magnitude, lower than those found by *Gatzemeier and Moorkamp* [2005] (more than two orders of magnitude). Our results suggest, for the first time, an emerging agreement between the two anisotropic coefficients with an electrical anisotropy most likely explained by hydrogen diffusion [*Gatzemeier and Tommasi*, 2006].

[31] This study confirms the agreement between the most conductive and the seismic fast-propagation directions at asthenospheric depths. In Central Germany, the present day plate motion determined by the HS2-Nuvel1 model [*Gripp and Gordon*, 1990] give a direction of 50°–55° which is not consistent with either the anisotropic direction in lithosphere (well resolved at 35°–40°) or in the asthenosphere (well resolved at 72°). Further work is required to understand these anisotropy directions.

[32] **Acknowledgments.** We acknowledge the Irish Center for High-End Computing (ICHEC) for providing computational facilities and support. This work was supported by a research grant from Science Foundation Ireland (SFI grant 07/RFP/GEOF759).

[33] The authors wish to thank the three anonymous reviewers.

References

Bischoff, M., B. Endrun, and T. Meier (2006), Lower crustal anisotropy in central Europe deduced from dispersion analysis of Love and Rayleigh waves, *Geophys. Res. Abstr.*, *8*, 10010.

Caldwell, T. G., H. M. Bibby, and C. Brown (2004), The magnetotelluric phase tensor, *Geophys. J. Int.*, *158*(2), 457–469, doi:10.1111/j.1365-246X.2004.02281.x.

Constable, S., T. J. Shankland, and A. Duba (1992), The electrical conductivity of an isotropic olivine mantle, *J. Geophys. Res.*, *97*, 3397–3404, doi:10.1029/91JB02453.

Deschamps, F., S. Lebedev, T. Meier, and J. Trampert (2008), Stratified seismic anisotropy reveals past and present deformation beneath the east-central United States, *Earth Planet. Sci. Lett.*, *274*, 489–498, doi:10.1016/j.epsl.2008.07.058.

Duba, A. G., and T. J. Shankland (1982), Free carbon and electrical conductivity in the Earth's mantle, *Geophys. Res. Lett.*, *9*, 1271–1274, doi:10.1029/GL009i011p01271.

Eaton, D. W., A. G. Jones, and I. J. Ferguson (2004), Lithospheric anisotropy structure inferred from collocated teleseismic and magnetotelluric observations: Great Slave Lake shear zone, northern Canada, *Geophys. Res. Lett.*, *31*, L19614, doi:10.1029/2004GL020939.

Eaton, D. W., F. Darbyshire, R. L. Evans, H. Grutter, A. G. Jones, and X. Yuan (2009), The elusive lithosphere-asthenosphere boundary (LAB) beneath cratons, *Lithos*, *109*, 1–22, doi:10.1016/j.lithos.2008.05.009.

Gatzemeier, A., and M. Moorkamp (2005), 3D modelling of electrical anisotropy from electromagnetic array data: Hypothesis testing for different upper mantle conduction mechanisms, *Phys. Earth Planet. Inter.*, *149*, 225–242, doi:10.1016/j.pepi.2004.10.004.

Gatzemeier, A., and A. Tommasi (2006), Flow and electrical anisotropy in the upper mantle: Finite-element models constraints on the effect of olivine crystal preferred orientation and microstructure, *Phys. Earth Planet. Inter.*, *158*, 92–106, doi:10.1016/j.pepi.2006.01.009.

Geissler, W. H., F. Sodoudi, and R. Kind (2010), Thickness of the central and eastern European lithosphere as seen by S receiver functions, *Geophys. J. Int.*, *181*, 604–634, doi:10.1111/j.1365-246X.2010.04548.x.

Gripp, A. E., and R. G. Gordon (1990), Current plate velocity to the hotspots incorporating the NUVEL-1 global plate motion model, *Geophys. Res. Lett.*, *17*, 1109–1112, doi:10.1029/GL017i008p01109.

Jones, A. G. (1982), On the electrical crust-mantle structure in Fennoscandia: No Moho and the asthenosphere revealed?, *Geophys. J. R. Astron. Soc.*, *68*, 371–388.

Jones, A. G., and I. J. Ferguson (2001), The electric Moho, *Nature*, *409*, 331–333, doi:10.1038/35053053.

Jones, A. G., P. Lezaeta, I. J. Ferguson, A. D. Chave, R. Evans, X. Garcia, and J. Spratt (2003), The electrical structure of the Slave craton, *Lithos*, *71*, 505–527, doi:10.1016/j.lithos.2003.08.001.

Karato, S. (1990), The role of hydrogen in the electrical conductivity of the upper mantle, *Nature*, *347*, 272–273, doi:10.1038/347272a0.

Kennett, B. L. N., E. R. Engdahl, and R. Buland (1995), Constraints on seismic velocities in the Earth from traveltimes, *Geophys. J. Int.*, *122*, 108–124, doi:10.1111/j.1365-246X.1995.tb03540.x.

Lebedev, S., B. Endrun, M. Bischoff, and T. Meier (2007), *Layering of seismic anisotropy and the past and present deformation on the lithosphere and asthenosphere beneath Germany*, paper presented at the XXIV General Assembly of the IUGG, Perugia, Italy.

Leibecker, J., A. Gatzemeier, M. Honig, O. Kuras, and W. Soyer (2002), Evidence of electrical anisotropic structures in the lower crust and the upper mantle beneath the Rhenish shield, *Earth Planet. Sci. Lett.*, *202*, 289–302, doi:10.1016/S0012-821X(02)00783-5.

Meier, T., K. Dietrich, B. Stoeckhert, and H.-P. Harjes (2004), One-dimensional models of shear wave velocity for the eastern Mediterranean obtained from the inversion of Rayleigh wave phase velocity and tectonic implications, *Geophys. J. Int.*, *156*, 45–58, doi:10.1111/j.1365-246X.2004.02121.x.

Moorkamp, M., A. G. Jones, and D. W. Eaton (2007), Joint inversion of teleseismic receiver functions and magnetotelluric data using a genetic algorithm: are seismic velocities and electrical conductivities compatible?, *Geophys. Res. Lett.*, *34*, L16311, doi:10.1029/2007GL030519.

Moorkamp, M., A. G. Jones, and S. Fishwick (2010), Joint inversion of receiver functions, surface wave dispersion and magnetotelluric data, *J. Geophys. Res.*, *115*, B04318, doi:10.1029/2009JB006369.

Savage, M. K. (1999), Seismic anisotropy and mantle deformation: what have we learned from shear wave splitting?, *Rev. Geophys.*, *37*, 65–106, doi:10.1029/98RG02075.

Simpson, F. (2002), Intensity and direction of lattice-preferred orientation of olivine: are electrical and seismic anisotropies of the Australian mantle reconcilable?, *Earth Planet. Sci. Lett.*, *203*, 535–547, doi:10.1016/S0012-821X(02)00862-2.

Smith, M. L., and F. A. Dahlen (1973), Azimuthal dependence of Love and Rayleigh-wave propagation in a slightly anisotropic medium, *J. Geophys. Res.*, *78*, 3321–3333, doi:10.1029/JB078i017p03321.

M. Bischoff, Institute of Geology, Mineralogy and Geophysics, Ruhr-University, D-44780 Bochum, Germany.

B. Endrun, Institute of Earth and Environmental Sciences, University Potsdam, Karl-Liebknecht Strasse 24, D-14476 Potsdam, Germany.

A. G. Jones and S. Lebedev, Dublin Institute for Advanced Studies, 5 Merrion Square, Dublin, Ireland.

T. Meier, Institute of Geosciences, Christian-Albrechts University, Otto-Hahn-Platz 1, D-24118 Kiel, Germany.

M. Moorkamp, Leibniz Institute of Marine Sciences at University of Kiel (IFM-GEOMAR), Wischofstrasse 1-3, D-24148 Kiel, Germany.

E. Roux, Institut de Ciències del Mar, CSIC, Passeig Maritim de la Barceloneta 37-49, E-08003 Barcelona, Spain. (roux@cmima.csic.es)